Exchange interactions and sensitivity of the Ni two-hole spin state to Hund's coupling in doped math xmlns="http://www.w3.org/1998/Math/MathML">msub>mi mathvariant="normal">NdNiO/mi>mn>2/mn>/msub>/math>

Xiangang Wan, Vsevolod Ivanov, Giacomo Resta, Ivan Leonov, and Sergey Y. Savrasov

Phys. Rev. B **103**, 075123 — Published 11 February 2021

DOI: 10.1103/PhysRevB.103.075123

Calculated Exchange Interactions and Sensitivity of Ni Two–Hole Spin State to Hund's Coupling in Doped $NdNiO_2$

Xiangang Wan*, Vsevolod Ivanov†, Giacomo Resta†, Ivan Leonov††, Sergey Y. Savrasov†
*National Laboratory of Solid State Microstructures,
School of Physics and Collaborative Innovation Center of Advanced Microstructures, Nanjing University, 210093 Nanjing
†Department of Physics and Astronomy, University of California, Davis, CA 95616 and
††M.N. Miheev Institute of Metal Physics, Russian Academy of Sciences and Ural Federal University, 620002 Yekaterinburg
(Dated: January 22, 2021)

Using density functional based LDA+U method and linear–response theory, we study the magnetic exchange interactions of the superconductor $Nd_{1-x}Sr_xNiO_2$. Our calculated nearest-neighbor exchange constant $J_1 = 82$ meV is large, weakly affected by doping and is only slightly smaller than that found in the sister compound $CaCuO_2$. We however find that the hole doping significantly enhances the inter–layer exchange coupling as it affects the magnetic moment of the Ni–$3d_{3z^2-r^2}$ orbital. This can be understood in terms of small hybridization of Ni-$3d_{3z^2-r^2}$ within the NiO_2 plane which results in a flat band near the Fermi level, and its large overlap along z direction. We also demonstrate that the Nd-$5d$ states appearing at the Fermi level, do not affect the magnetic exchange interactions, and thus may not participate in the superconductivity of this compound. Whereas many previous works emphasize the importance of the Ni-$3d_{x^2-y^2}$ and Nd-$5d$ orbitals, we instead analyze the solution of Ni-$3d_{x^2-y^2}$/Ni-$3d_{3z^2-r^2}$ minimal model using Dynamical Mean Field Theory. It reveals an underlying Mott insulating state which, depending on precise values of the intra–atomic Hund's coupling less or larger than 0.83 eV, selects upon doping either S=0 or S=1 two–hole states at low energies leading to very different quasiparticle band structures. We propose that trends upon doping in spin excitational spectrum and quasiparticle density of state can be a way to probe Ni $3d^8$ configuration.

PACS numbers:

I. INTRODUCTION

Since the discovery of high–temperature superconductors (HTSCs)[1], tremendous theoretical and experimental efforts have been devoted to understanding the novel physics of this family of compounds[2–4]. All HTSCs are comprised of quasi–two–dimensional CuO_2 planes separated by charge reservoir spacer layers, and their parent compounds have antiferromagnetic (AFM) order with very strong in–plane magnetic exchange interactions, belonging to the class of charge–transfer insulators[5]. Upon doping, holes occupy the O–$2p$ orbital, and due to the strong hybridization between Cu–$3d_{x^2-y^2}$ and O–$2p$ orbitals, a Zhang–Rice singlet is formed[6]. It has been widely accepted that the HTSCs can be described by an effective single band t–J model, with different parameters explaining the variation in T_c in different materials [7, 8].

Inspired by HTSCs, the search for possible novel superconducting behavior in nickelates has been attracting significant attention, as their structure and electronic configuration is similar to that of the cuprates [9–12]. Unfortunately, the monovalent Ni ion is strongly unstable and scarcely formed in mineral compounds, making, for example, $LaNiO_2$ difficult but possible to synthesize[10]. First–principles Local Density Approximation (LDA) based calculations revealed an important difference between $LaNiO_2$ and its sister infinite–layer HTSC compound $CaCuO_2$: the Fermi surface of $CaCuO_2$ consists of only one two–dimensional band, while $LaNiO_2$ seems quite three–dimensional, with La–derived $5d$ states and Ni–$3d$ states crossing the Fermi level[13]. Numerical calculations predicted AFM magnetic order[13, 14], but magnetization and neutron powder diffraction observe no long–range order in $LaNiO_2$[11]. At high temperatures (150K < T < 300K), the susceptibility of $LaNiO_2$ can be fitted by the sum of a temperature independent term, and a Curie–Weiss $S = \frac{1}{2}$ paramagnetic term with a large Weiss constant ($\theta = -257$K), indicating a significant correlation between Ni spins[11]. $LaNiO_2$ shows metallic behavior, but resistivity increases at lower temperatures and no superconducting state has been observed [9–11].

Recently, $Nd_{0.8}Sr_{0.2}NiO_2$ thin films were synthesized on a $SrTiO_3$ substrate using soft–chemistry topotactic reduction, and superconductivity with considerably high T_c (up to 15K) was observed[15]. The superconducting phase displays a doping–dependent dome for $Nd_{1-x}Sr_xNiO_2$ ($0.125 < x < 0.25$), which is remarkably similar to that of the cuprates [16, 17]. Very recently, superconductivity has also been observed in doped $PrNiO_2$[18].

These breakthroughs have stimulated large–scale theoretical efforts to understand the nature of the superconductivity in rare–earth nickelates. LDA band structures [19] predict that both Nd–$5d$ and Ni–$3d_{x^2-y^2}$ orbitals contribute significantly to the Fermi surface of parent compound $NdNiO_2$. Most calculations treat the three $4f$ electrons in Nd^{3+} as core electrons, although the role of Nd–$4f$ has been emphasized recently[20]. Many–body

perturbative GW calculations result in almost no modification to the Fermi–surface topology and its orbital composition[21]. Focusing on the Fermi surface, different minimal models have been proposed to describe the low energy physics of this material using a Wannier function approach, including: a three–band model with Ni-$3d_{x^2-y^2}$, Nd–$5d_{3z^2-r^2}$ and an interstitial s orbital[22]; a three–band model with Ni–$3d_{x^2-y^2}$, Nd–$5d_{3z^2-r^2}$ and Nd–$5d_{xy}$[23, 24]; a two–band model with Ni–$3d_{x^2-y^2}$ and Nd–$5d_{3z^2-r^2}$[25, 26]; and a four–band model[27]. The effect of topotactic hydrogen has been discussed as well[28].

Several works addressed strong correlation effects among Ni 3d electrons [29]–[46] Due to a large energy difference between O–$2p$ and Ni–$3d$ levels, the undoped $NdNiO_2$ has been suggested to be a Mott insulator, and a coexistence/competition between low energy S=0 and S=1 states has been proposed for the hole doped case [29] where some Ni ions would acquire a formal $3d^8$ configuration. The origin of these two–hole states has been discussed in a recent literature[30–35]. As it is commonly accepted that the undoped Ni $3d^9$ configuration corresponds to the hole of x^2-y^2 symmetry, the two–hole states produced by doping can either end up as intraorbital singlets or interorbital triplets. It has been first pointed out[29] that the S=1 state maybe incompatible with robust superconductivity, and indeed exact diagonalization study of Ni impurity embedded into the oxygen environment [29] as well as a number of many–body calculations using a combination of LDA with Dynamical Mean Field Theory (DMFT)[30, 33] pointed to the formation of the intraorbital singlets.

The first–principles physics of competing Ni-$3d_{x^2-y^2}$ vs. Ni–$3d_{3z^2-r^2}$, and the connected issue of having the Ni–$3d_{3z^2-r^2}$ states at the Fermi level with hole doping has been first put forward in Ref. [34]. In addition, the role of Ni-$3d_{x^2-y^2}$ and Ni-$3d_{3z^2-r^2}$ orbitals has been emphasized in Ref. [30]. A recent GW+DMFT work [36], highlighted Ni-$3d_{3z^2-r^2}$ flat–band physics as well as Ref. [37]. Furthermore, a variant of the t–J model with S=1 has been proposed and shown to exhibit d–wave superconductivity[32]. Symmetries of the pairing states based on a two–orbital Ni-$3d_{x^2-y^2}$/Ni-$3d_{xy}$ model Hamiltonian with competing S=0 and S=1 two–hole states have been discussed[31]. DMFT calculations for the two–orbital Ni–$3d_{x^2-y^2}$/Ni–$3d_{3z^2-r^2}$ system argued that a multiorbital description of nickelate superconductors is necessary [35]. Excitations and superconducting instabilities have also been explored by a random phase approximation [38]and by a variant of the t-J model[39]. Local spin, charge and orbital susceptibilities have been calculated using a combination of DMFT with a local quasiparticle self–consistent GW method and emphasized the Hund's physics of Ni–e_g electrons[40].

No sign of magnetic order has been observed in the original report on superconductivity in $NdNiO_2$[15], which may be attributed to defects, such as unwanted hydrides or hydroxides that might form as by–products of the creation of the rare Ni^+ oxidation state during the synthesis of this compound. Another consideration is that $LaNiO_3$ is close to an antiferromagnetic quantum critical point (QCP)[47], therefore it is reasonable to expect that with lower dimensionality, $NdNiO_2$ would pass the QCP and display magnetism. Very recently, strong spin fluctuations and considerable AFM exchange interactions have been observed in $NdNiO_2$[48] as well as nuclear magnetic resonance (NMR) data [49] provided an addtional evidence for quasi–static AFM order below 40 K and dominant spin fluctuations at higher temperatures in $Nd_{0.85}Sr_{0.15}NiO_2$ bulk materials. The exchange interactions have also been discussed in several works [23, 50–52]. The calculated electron–phonon interaction ($\lambda \leq 0.32$) is too small to explain the 15K T_c in this material[22], meaning the spin excitations, which are thought to be responsible for the superconductivity in HTSCs[2–4], are worth careful investigation.

In this work, based on a density functional LDA+U method and linear–response theory[53], we perform detailed studies of exchange interactions for both parent and doped $NdNiO_2$. The method does not rely on a total energy analysis, and instead directly computes the exchange constant for a given wave vector $\mathbf{q}$ based on the result of the magnetic force theorem [54]. Our results show that although the Fermi surface of undoped $NdNiO_2$ is quite three–dimensional, its magnetic exchange interaction J has a clear two–dimensional feature with large in–plane $J_1 = 82$ meV and much smaller out–of–plane J_{z1}. However, the Ni–$3d_{3z^2-r^2}$ band close to the Fermi level is quite flat, therefore within the LDA+U method for a reasonable range of the values of Hubbard U above 4 eV, holes introduced by doping preferentially occupy the Ni–$3d_{3z^2-r^2}$ orbitals while Ni–t_{2g} states remain remarkably inert. The in–plane J_1 remains largely unaffected by doping, but the magnetic moment of the Ni–$3d_{3z^2-r^2}$ orbital and the out–of–plane J_{z1} both grow significantly in accord with recent findings[37] Our calculation using a constrained–orbital–hybridization method [55] unambiguously demonstrates that while Nd–$5d$ makes an important contribution to the Fermi surface, it has almost no effect on the magnetic exchange interaction. It is expectable result, since it is known that Nd-5d orbitals have negligible hybridization with Ni orbitals [22, 56]. This means the magnetic excitations in hole–doped $NdNiO_2$ can be described by an effective model including Ni–$3d_{x^2-y^2}$/Ni–$3d_{3z^2-r^2}$ orbitals whose role has been emphasized in many recent works [19]–[46].

To gain additional insight, we discuss the solutions of such two–band model on the basis of Dynamical Mean Field Theory using the parameters deduced from our band structure calculations. In contrast to the static mean field description, such as LDA+U, where holes occupying Ni–$3d_{3z^2-r^2}$ states promote interorbital triplets, whether S=0 or S=1 state emerges from our DMFT sim-

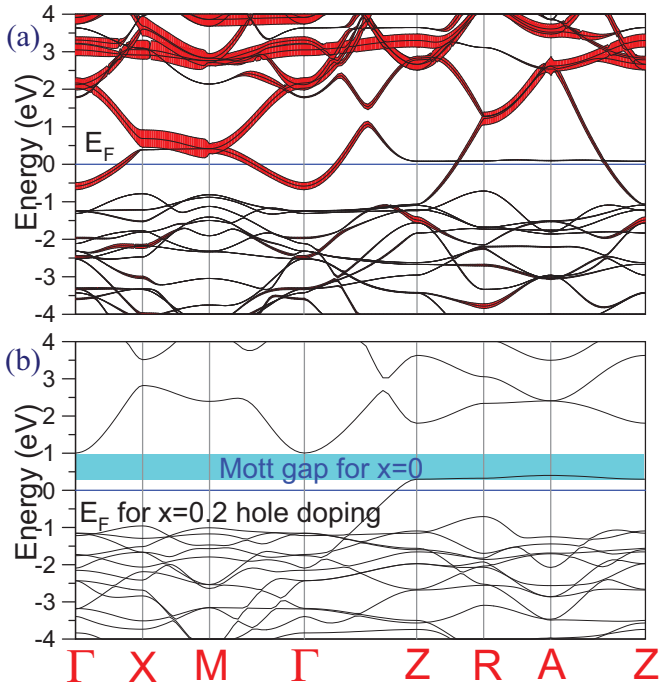

FIG. 1: Band structure of (π,π,0) AFM ordered $NdNiO_2$ from LDA+U calculations with $U = 6.0$ eV. (a) undoped $NdNiO_2$ with Nd–5d oribtal character shown in red, (b) constrained orbital-hybridization calculation for $NdNiO_2$ with the Nd–5d band shifted up by 2 Ry. The position of the Fermi level corresponds to 0.2 hole doping.

ulation depends on a precise value of the intraatomic Hund's coupling J_H in the vicinity of its commonly accepted range of values 0.5–1 eV. This leads to very different quasiparticle band structures. We thus propose that trends upon doping in magnetic exchange interactions and quasiparticle density of states can be a way to probe Ni $3d^8$ configuration.

Our paper is organized as follows. In Section II we describe our LDA+U and constrained–orbital–hybridization calculations for the exchange interactions. In Section III, we discuss a minimal two–band model that emerges from our study and its solution based on Dynamical Mean Field Theory. Section IV is the conclusion.

II. CALCULATIONS OF EXCHANGE INTERACTIONS

We perform our density functional based electronic structure calculations within the full potential linear–muffin–tin–orbital (LMTO) method[57]. To take into account the effect of on–site electron–electron interactions between Ni–3d orbitals we add a correction due to Hubbard U using the so–called LDA+U approach[58]. Although, the experimental situation on magnetism in nickelates is still unclear, hinted by the cuprate physics,

TABLE I: Calculated exchange interactions, J_1, J_2 (in-plane nearest, next-nearest) and J_{z1}, J_{z2} (out-of-plane nearest, next-nearest) in meV for various hole dopings x. Positive/negative sign denotes AFM/FM interaction. We also list the calculated total magnetic moment at the Ni site, M_{tot}, and magnetic moment at the Ni-3$d_{3z^2-r^2}$ orbital, $M_{3z^2-r^2}$, (in μ_B).

x	J_1	J_2	J_{z1}	J_{z2}	M_{tot}	$M_{3z^2-r^2}$
0.00	82.24	-4.84	-3.40	-23.00	0.97	0.17
0.05	71.84	-5.08	-21.40	-22.40	1.03	0.23
0.10	65.88	-5.68	-39.36	-18.48	1.07	0.27
0.15	64.60	-4.68	-59.04	-11.08	1.08	0.30
0.20	58.20	-4.16	-80.88	-5.56	1.15	0.35
0.25	57.36	-2.84	-97.36	-4.84	1.16	0.38
0.30	50.76	-2.16	-105.52	-2.88	1.23	0.44

an assumption of the AFM ordered state in the parent compound should be a good starting point for a theoretical modeling. Ultimately, if AFM spin fluctuations in the doped state are responsible for superconductivity, the exchange interactions in the ordered state set the scale for those fluctuations, which justifies this assumption and provides the basis for our static linear response calculation of J's. An alternative measure of those spin fluctuations would be a full calculation of wavevector and frequency dependent spin susceptibility directly in paramagnetic state. Although possible, in principle, it is a lot more involved and goes beyond the scope of this work.

We vary the parameter U for Ni–3d between 4.0 and 8.0 eV, and find that the essential properties and our conclusions do not depend on the value of U in this range[59]. Below we report our results for exchange constants with $U = 6$ eV and Hund's $J_H = 0.95$ eV. Experimental lattice parameters have been used[15].

The magnetic exchange interactions $J(\mathbf{q})$ were evaluated assuming a rigid rotation of atomic spins, using a previously developed linear–response approach [53]. This technique has been applied successfully to evaluate exchange interactions for a series of materials, including transition–metal oxides[53], HTSCs[60], Fe–based superconductors[61]; europium monochalcogenides[62], orbital–ordered noncollinear spinel MnV_2O_4[63], and Dirac magnon material Cu_3TeO_6[64]. We also use a constrained–orbital–hybridization method to provide theoretical insights into the various contributions[55] to the exchange interactions in hole doped $NdNiO_2$. To avoid the effect of the very narrow Nd–4f bands, we shift the three occupied Nd–4f orbitals downward while shifting the rest of the Nd–4f band upward by using a constrained–orbital approach [55]. Since the obtained results do not depend on the magnitude of the shifts, we display the results with the Nd–4f bands shifted by ± 2.0 Ry.

Similarly to previously reported band structure calculations for $LaNiO_2$[13, 22, 24, 27], there are two bands

TABLE II: Calculated exchange interactions (in meV) for x=0.2 hole doped $NdNiO_2$, with Nd-5d shifted upward by various energies (in Ry).

Shift (Ry):	J_1	J_{z1}
0.05	64.28	-84.04
0.10	65.48	-83.76
0.50	69.68	-75.52
2.00	71.92	-78.96

crossing the Fermi level in the LDA band structure of $NdNiO_2$, with one band primarily derived from the Ni–$3d_{x^2-y^2}$ orbital and the other consisting of predominantly Nd–5d character. Just as with $LaNiO_2$[13, 22], there is a gap between Ni–3d and O–2p bands (around -3.5 eV). Moreover, Ni–O bond length in $NdNiO_2$ (1.96 $\AA$) is slightly larger than the Cu–O bond length in $CaCuO_2$ (1.92 $\AA$). Thus the bandwidth of the Ni–$3d_{x^2-y^2}$ band correspondingly smaller than that of the Cu–$3d_{x^2-y^2}$ band. While in both $NdNiO_2$ and $CaCuO_2$, the $3d_{3z^2-r^2}$ orbitals have very small dispersions along the $ZRAZ$ line, the dispersion of the Ni–$3d_{3z^2-r^2}$ state along ΓZ is considerably larger than that of Cu–$3d_{3z^2-r^2}$. Moreover, compared to Cu–$3d_{3z^2-r^2}$, the Ni–$3d_{3z^2-r^2}$ band lies closer to the Fermi level. These two features are expected to significantly affect the magnetic behavior in the hole doped $NdNiO_2$.

We now perform the LDA+U calculation to examine magnetic exchange interactions in undoped $NdNiO_2$. Our results show that the exchange coupling is large for the nearest–neighbor J_1 within the NiO_2 plane. The sign of this term is AFM, and thus the NiO_2 layer shows a (π,π) spin ordering. There is some debate about the magnitude of the exchange interaction, with estimates ranging from much less than that of cuprates [23, 29, 50] to comparable to the value of exchange interaction in $CaCuO_2$[26, 51, 52]. Our calculated value of J_1 is 82.24 meV as referenced to the form of the Heisenberg Hamiltonian

$$H = \frac{1}{2}\sum_{ij} J_{ij}\mathbf{S}_i\mathbf{S}_j \qquad (1)$$

with S=1/2. The estimate of J_1 =25 meV from the Raman scattering experiment of the two–magnon peak [48, 50] is significantly smaller. Recent resonance X–ray scattering experiments performed for trilayer nickelate $La_4Ni_3O_8$ report this value to be 69 meV[65]. The in–plane J_1 that we compute is only about 25% less than that found in $CaCuO_2$[60]. We attribute it to a smaller Ni–3d and O–2p hybridization and larger energy splitting between Ni–3d and O–2p as has previously been pointed out[13]. Consistent with the result of (π,π,0) spin ordering being slightly more energetically favorable than (π,π,π), our calculation produces a small out–of–plane FM exchange interaction, with nearest neighbor $J_{1z} = -3.4$ meV and second nearest neighbor $J_{2z} = -23$ meV, respectively. Our calculations reveal that the magnetic moment at the Ni site (0.97 μ_B), residing mostly in the $3d_{x^2-y^2}$ orbital, is much larger than that at Cu sites in HSTCs.

There exists a fairly flat band right at the Fermi level along the $ZRAZ$ line, in the band structure of the magnetic ground state configuration of $NdNiO_2$, as shown in Fig.1(a). This flat band has predominantly Ni–$3d_{3z^2-r^2}$ character, and plays an important role when hole doping is considered. The very small in–plane dispersion of the Ni–$3d_{3z^2-r^2}$ band can be understood as a consequence of the symmetry of the Ni–$3d_{3z^2-r^2}$ orbital, which can only weakly hybridize with the neighboring O–2p.

To examine the doping dependence we perform a series of hole–doped calculations, varying the number of holes per unit cell from 0.05 to 0.30 by using the virtual crystal approximation. These calculations show that the hole doping within this range does not significantly change the shape of the band structure apart from shifting the Fermi level downward. Regardless of the hole–doping concentration, the Ni–t_{2g} band is almost fully occupied and does not contribute to the magnetic moment. The magnetic moment of the Ni–$3d_{x^2-y^2}$ orbital is also unaffected by the hole doping. Instead, the holes preferentially occupy the flat Ni–$3d_{3z^2-r^2}$ band, and, as a result, the magnetic moment of this orbital increases with doping as shown in Table I. Noting the considerable Ni–$3d_{3z^2-r^2}$ band dispersion along ΓZ, and the formation of magnetic moments in this orbital, one can expect the emergence of out–of–plane magnetic exchange interactions. This result has been confirmed by our linear response calculation. As shown in Table I, hole doping significantly enhances the out–of–plane J_{z1}, while the in–plane J_1 remains mostly unaffected.

The 5d orbital is spatially very wide, and can have a crucial effect on the magnetic exchange interaction through 4f–5d hybridization, even though it is empty and located above the Fermi level[62]. In $NdNiO_2$, the Nd–5d band appears at the Fermi level, making it important to understand the role of the Nd–5d orbital in magnetic exchange interactions. We address this issue by using a constrained–orbital–hybridization approach[55]. We perform the calculations with the Nd–5d band shifted upward by various values. Fig. 1(b) shows the band structure for the case where the Nd–5d band is shifted upward by 2 Ry. As one can see, the AFM insulating state emerges from this calculation for the undoped case, while hole doping vacates the Ni–$3d_{3z^2-r^2}$ band within $k_z = \pi/c$ plane.

Our calculation shows that both in–plane J_1 and out–of–plane J_{z1} exchange interactions are not sensitive to the position of the Nd–5d band as shown in Table II, clearly indicating that the effect of this orbital on the magnetic exchange interactions is negligible. A similar calculation was performed for $LaNiO_2$ to further confirm these findings[59]. While the obtained values of the ex-

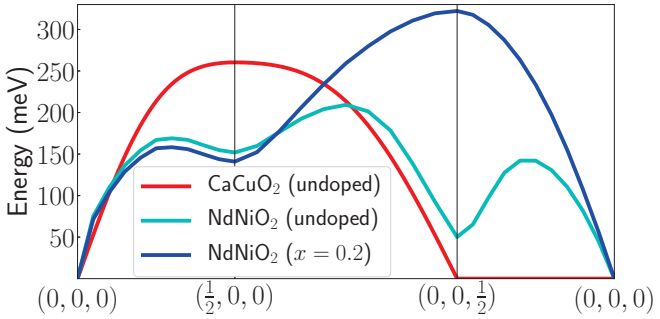

FIG. 2: Calculated spin–wave dispersions for the undoped $NdNiO_2$ (cyan), and 0.2 hole-doped $NdNiO_2$ (blue), with U=6eV. For comparison, we also plot the results of $CaCuO_2$ (red)[60].

change interactions are slightly different, the key features discussed above are the same.

We illustrate the effect of increasing out–of–plane exchange interactions in doped $NdNiO_2$, using an antiferromagnetic Heisenberg model, Eq. (1). Its linear spin–wave dispersion is given by

$$\omega(\mathbf{q}) = S\sqrt{[J_{11}(\mathbf{q}) - J_{11}(0) + J_{12}(0)]^2 - [J_{12}(\mathbf{q})]^2}$$

where $J_{11}(\mathbf{q})/J_{12}(\mathbf{q})$ are the exchange interactions within the same/different sublattices. (A quantum correction factor $Z_c \approx 1.18$ which is sometimes used [60] in front of this formula is omitted here) We plot these dispersions in Fig. 2 for both undoped and 0.2 hole–doped $NdNiO_2$ in Fig. 2, along with those of $CaCuO_2$ for comparison[60]. We utilize our calculated exchange constants as a function of the wavevector for this purpose, and not their nearest neighbor fits shown in Table I. This procedure fully accounts for the long–range effects of the interactions. Our model demonstrates some differences between the spin–wave dispersions of $NdNiO_2$ and $CaCuO_2$. Notably, the peak around $(\frac{1}{2}, 0, 0)$ is reduced in $NdNiO_2$ compared with $CaCuO_2$, as a consequence of the smaller in–plane exchange couplings, and is largely unaffected by doping. In contrast, the out–of–plane exchange interactions strongly depend on doping, which can be seen in the changing dispersion along ΓZ. In undoped $NdNiO_2$, an out–of–plane J_{z2} dominates over the vanishing nearest neighbor J_{z1}. Doping amplifies J_{z1} while suppressing J_{z2}, resulting in the disappearance of the valley at $(0, 0, 1/2)$ in the dispersion. Thus, in contrast with HTSCs, our calculation of J's here predicts a strongly doping dependent resonance that could in principle be observed in neutron experiments.

III. TWO–BAND MODEL

A minimal model for the electronic structure of $NdNiO_2$ that emerges from the present study should involve Ni–$3d_{x^2-y^2}$ and Ni–$3d_{3z^2-r^2}$ orbitals only. Their

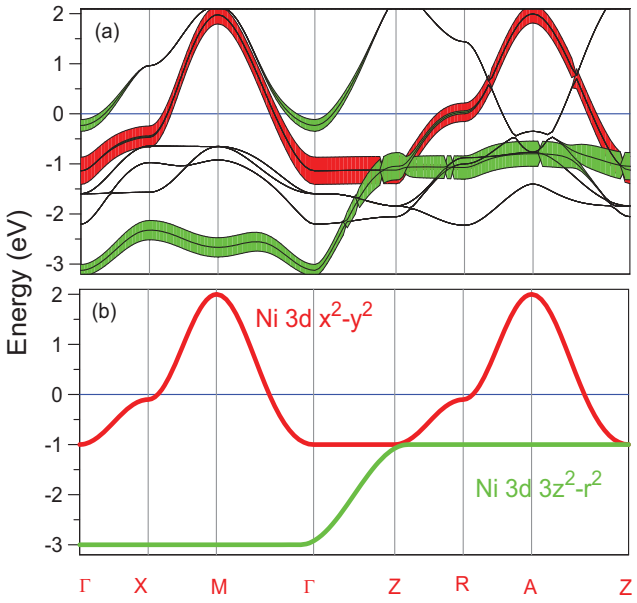

FIG. 3: (a) Non–magnetic LDA band structure of $NdNiO_2$ with the orbital character of Ni-$3d_{x^2-y^2}$ and Ni-$3d_{3z^2-r^2}$ states shown in red and green, respectively. (b) The corresponding two-band tight–binding model[59].

role has already been emphasized in many recent works[19]–[46] and, as we argue here, their importance is based on sensitivity of magnetic excitations to the position of various orbitals. The parameters of the model can be obtained by tracing the orbital character of these states from the non–magnetic LDA calculation. We show this in red for Ni–$3d_{x^2-y^2}$ and in green for Ni–$3d_{3z^2-r^2}$ in Fig. 3(a). The derived two–band tight–binding model is illustrated in Fig. 3(b). In the large U limit, such model at a quarter filling by holes (3 electron filling) is expected to exhibit a Mott insulator for $3d_{x^2-y^2}$ band, with the lower Hubbard band placed below $3d_{3z^2-r^2}$ state. Its antiferromagnetic solution in the Hartree–Fock approximation will result in the band structure very similar to the LDA+U result shown in Fig. 1(b), which also assumes that the t_{2g} states of Ni, although appear in the same energy range, are apparently irrelevant. According to our LDA+U calculation with $U \gtrsim 4$ eV, doping sends the holes primarily to the $3d_{3z^2-r^2}$ state promoting interorbital triplets. This is seen in Fig. 1(b) where the Fermi level shifting downwards unoccupies the $3d_{3z^2-r^2}$ band in $k_z = \pi/c$ plane which explains doping dependence of the orbital occupancies shown in Table I.

The described picture should however be contrasted to the genuine strong correlation effect that prompts to consider an additional hole to be injected into either Ni $x^2 - y^2$ or $3z^2 - r^2$ orbital resulting either in an intraorbital singlet or interorbital triplet. This is different from cuprates, where holes end up in low–lying O 2p band forming Zhang–Rice singlet states[6]. Here, it is not the

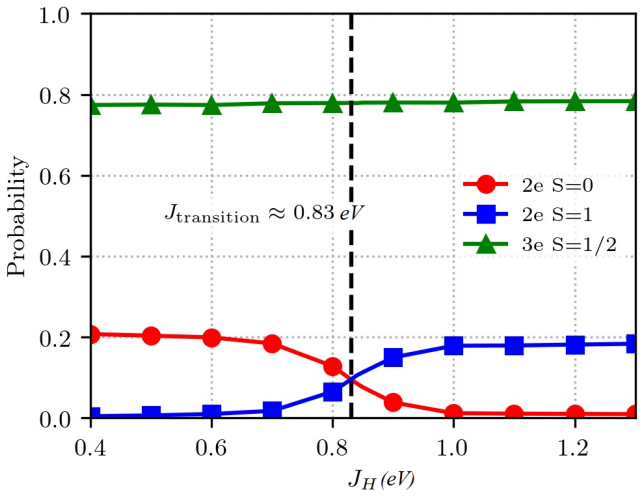

FIG. 4: Calculated probabilites for the three electron S=1/2 and two–electron S=0 and S=1 states as a function of Hund's coupling J_H using Dynamical Mean Field Theory and Continious Time Quantum Monte Carlo Method for the two–band model of $NdNiO_2$ corresponding to doping by 0.2 holes (filling by 2.8 electrons in the model). An inverse temperature of $\beta = 40$ is used in the calculations.

relation of Hubbard U to the crystal field splitting Δ between x^2-y^2 and $3z^2-r^2$ levels but the competition of the Hund's rule J_H and Δ which should be examined to understand the origin of the two–hole state in the doped case[29, 30, 33–35]. To illustrate the proximity of both (S=0 and S=1) solutions, a simple diagonalization of the $3d^8$ shell with U=6 eV and our deduced from Fig. 1(b) crystal field splitting Δ=2.2 eV reveals that the lowest energy state is S=0 for $J_H < 0.9$ eV, and S=1 otherwise. This value is well within the range of generally assumed Hund's rule exchange energies for transition metal oxides and highlights a delicate balance in extracting the two–hole ground state configuration.

Although a number of full–fledge multiorbital LDA+DMFT calculations have been recently carried out to understand the many–body physics of doped $NdNiO_2$[30, 33, 43], a strong sensitivity of the solution to the input parameters, such as J_H, is expected. This has been already highlighted in the earlier work simulating two semicircular densities of states with the crystal field splitting as a parameter [35]. To gain a further qualitative insight, here we study our derived two–band model using Dynamical Mean Field Theory[66] and Continuous Time Quantum Monte Carlo method[67]. The parameters U=6 eV and Δ=2.2 eV are fixed while J_H is adjusted. The undoped case of Ni $3d^9$ S=1/2 state corresponds to the electronic filling equal to 3 in this model, where we easily recover a paramagnetic Mott insulating state with the gap of the order of U that opens up in the x^2-y^2 band and with the $3z^2-r^2$ states that remain completely occupied. Doping this model with 0.2 holes (filling by 2.8 electrons) results in finite probability to find either S=0 or S=1 states in addition to S=1/2 that depends on J_H. These probabilities extracted from the Quantum Monte Carlo simulation are shown in Fig. 4 very close to our earlier estimate of 0.9 eV.

Our results for the **k**–resolved spectral functions are summarized in Fig. 5, where a comparative study is presented for the two quasiparticle band structures corresponding to S=0 state (J_H is set to 0.6 eV, Fig. 5(a)) and to S=1 state (J_H is set to 1 eV, Fig. 5(b)). One can see from the calculated spectrum for J_H =0.6 eV that the $3z^2-r^2$ state remains completely occupied while the doping primarily affects the x^2-y^2 band which now shows a typical for DMFT three–peak structure with the two Hubbard bands appearing below and above the Fermi level and a renormalized quasiparticle band that crosses E_F. The k dispersion for all three features is similar to the original dispersion of the x^2-y^2 band.

A different picture emerges from the calculation with $J_H = 1$ eV shown in Fig. 5(b). In this case, renormalized quasiparticles of the $3z^2-r^2$ character appear at the Fermi level which illustrate the formation of the interorbital triplet states. A very strong peak in the quasiparticle density of state is expected to be present at E_F due to the non–dispersive portion of the $3z^2-r^2$ band within the ZRA plane. At the same time, the x^2-y^2 band does not develop a three–peak structure and is characterized by the two Hubbard bands as in the undoped case. A very similar behavior has been already predicted in a recent work[34] where it was termed as the "Kondo resonance" property, carried by the Ni-$3z^2-r^2$ character.

Our previous LDA+DMFT calculations [43] performed for $J_H = 0.95$ eV are in somewhat agreement with this result although the appearance of the flat band was detected by us earlier only at a higher doping (˜0.4). The origin of this discrepancy may lie in a more complex interplay between crystal fields and double counting effects in a self–consistent multiorbital simulation or in an analytical continuation of the QMC derived spectral functions resulting in a smaller and/or more broadened spectral weight as compared to the result of the model. We have additionally checked the probabilities of various spin states within LDA+DMFT and they are mostly in line with what we observe in Fig. 4.

Since the Hund's coupling J_H of 0.8 to 0.9 eV is well within the range of commonly accepted values, we cannot make a definite conclusion about whether S=0 or S=1 scenario is realized for doped nickelates. However, possible future angle–resolved photoemission (ARPES) experiments may provide important insight since as illustrated by our calculations the quasiparticle band structure is very different between the two cases. Furthermore, while ARPES spectra in the hole–doped HTSCs show waterfall–like behavior[68], we do not expect waterfalls to appear here due to a lack of oxygen states at energies close to E_F and associated physics responsible

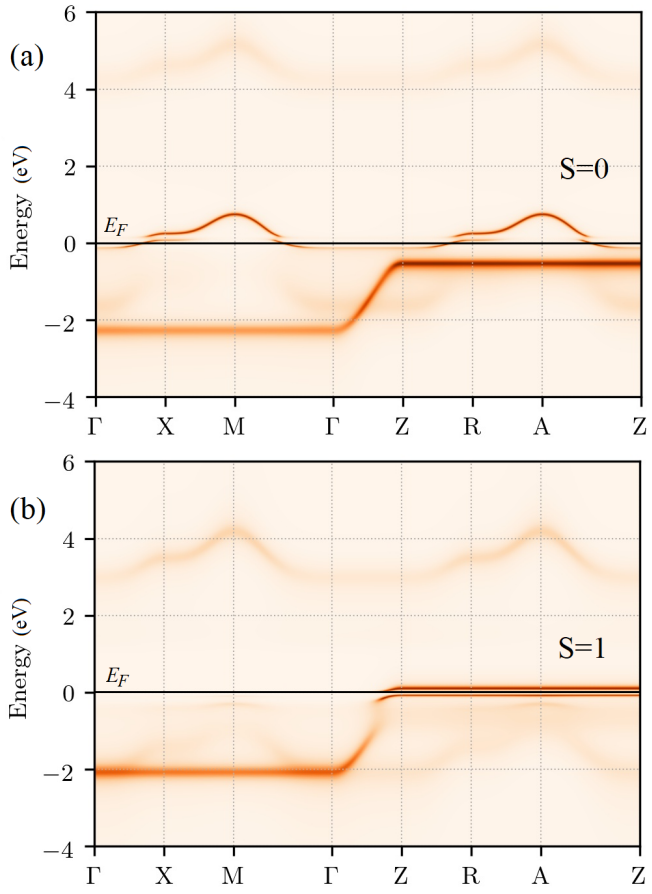

FIG. 5: Quasiparticle band structures of the two– band model of $NdNiO_2$ obtained by Dynamical Mean Field Theory and Continious Time Quantum Monte Carlo Method for the doping level of 0.2 holes: (a) Calculation for Hund's coupling $J_H = 0.6$ eV that corresponds to S=0 two–hole state; (b) Calculation for $J_H = 1$ eV corresponding to S=1 two-hole state. An inverse temperature $\beta = 40$ is used for the calculations.

for the formation of the low energy states[69].

IV. CONCLUSION

In conclusion, using the LDA+U method, we have calculated magnetic exchange interactions for the doped $NdNiO_2$ novel superconductor. We find that the parent compound is mostly two–dimensional, with large nearest neighbor in–plane, and small out–of–plane exchange interactions. Upon doping, the out–of–plane coupling J_{z1} was found to increase dramatically, while the in–plane J_1 is almost unchanged. To clarify the origin of these trends, we analyzed the symmetry of the holes induced by doping which were found to be primarily of the $3d_{3z^2-r^2}$ character promoting the formation of interorbital triplet as Ni $3d^8$ ground state configuration. We also investigated the role of the Nd–$5d$ states, which contribute substantially to the Fermi surface of $NdNiO_2$. Shifting this band upward using a constrained–orbital–hybridization method has little effect on exchange interactions, which leads us to conclude that Nd–$5d$ states have negligible effect on the spin fluctuations and the superconductivity in $NdNiO_2$. A minimal two–band model with active Ni–$3d_{x^2-y^2}$ and Ni–$3d_{3z^2-r^2}$ orbitals has been further studied with DMFT to reveal an underlying Mott insulating state which upon doping selects either S=0 and S=1 two–hole states depending on the Hund's coupling in the range of its commonly accepted values 0.8 to 0.9 eV. Should S=1 state be valid, we rely on our LDA+U result to predict that upon doping the spin susceptibility gains three dimensionality as it gets enhanced along ΓZ. This can be readily observed in neutron experiments and can be one way to probe the two–hole configuration. We also rely on our DMFT result to predict a formation of a strong quasiparticle peak at the Fermi level detectable by ARPES experiments. A small anisotropy in H_{c2} was indeed discovered very recently [70] illustrating the three–dimensional nature of $NdNiO_2$ which starkly contrasts with the two–dimensional superconductivity in HTSCs. At the same time, most recent x–ray absorption spectroscopy (XAS) and resonant inelastic x-ray scattering (RIXS) experiments are found to be consistent with a d^8 spin singlet state [71]. These results should be important in future studies of nickelate superconductors.

ACKNOWLEDGEMENTS

X.W. is supported by the NSFC (Grants No. 11834006, No. 11525417, No. 51721001, and No. 11790311), National Key R&D Program of China (Grants No. 2018YFA0305704 and No. 2017YFA0303203) and by 111 Project. X.W. also acknowledges the support from the Tencent Foundation through the XPLORER PRIZE . V.I, G.R. and S.Y.S are supported by NSF DMR Grant No. 1832728. I.L. acknowledges support by the Russian Foundation for Basic Research (Project No. 18-32-20076). The DMFT electronic structure calculations were supported by the state assignment of Minobrnauki of Russia (theme "Electron" No. AAAA-A18-118020190098-5).

[1] J. G. Bednorz and K. A. Müller, Possible high Tc superconductivity in the Ba-La-Cu-O system, Zeitschrift fur Physik B Condensed Matter **64**, 189 (1986).
[2] C. C. Tsuei and J. R. Kirtley, Pairing symmetry in cuprate superconductors, Rev. Mod. Phys. 72, 969 (2000).
[3] D. J. Scalapino, A common thread: The pairing interaction for unconventional superconductors, Rev. Mod.

Phys. **84**, 1383 (2012).
[4] P. A. Lee, N. Nagaosa, and X.-G. Wen, Doping a Mott insulator: Physics of high-temperature superconductivity, Rev. Mod. Phys. **78**, 17 (2006).
[5] J. Zaanen, G. A. Sawatzky, and J. W. Allen, Band gaps and electronic structure of transition-metal compounds, Phys. Rev. Lett. **55**, 418 (1985).
[6] F. C. Zhang and T. M. Rice, Effective Hamiltonian for the superconducting Cu oxides, Phys. Rev. B **37**, 3759(R) (1988).
[7] E. Pavarini, I. Dasgupta, T. Saha-Dasgupta, O. Jepsen, and O. K. Andersen, Band-Structure Trend in Hole-Doped Cuprates and Correlation with T_{cmax}, Phys. Rev. Lett. **87**, 047003 (2001).
[8] H. Sakakibara, H. Usui, K. Kuroki, R. Arita, and H. Aoki, Two-Orbital Model Explains the Higher Transition Temperature of the Single-Layer Hg-Cuprate Superconductor Compared to That of the La-Cuprate Superconductor, Phys. Rev. Lett. **105**, 057003 (2010).
[9] J. Choisnet, R.A. Evarestov, I.I. Tupitsyn and V.A. Veryazov, Investigation of the chemical bonding in Nickel mixed oxides from electronic structure calculations, J. Phys. Chem. Solids **l57**, 1839 (1996).
[10] M.J. Martínez-Lope, M.T. Casais, J.A. Alonso, Stabilization of Ni^{+} in defect perovskites $La(Ni_{1-x}Al_x)O_{2+x}$ with 'infinite-layer' structure, J. Alloys and Compounds **275**, 109 (1998)
[11] M. A. Hayward, M. A. Green, M. J. Rosseinsky, and J. Sloan, Sodium Hydride as a Powerful Reducing Agent for Topotactic Oxide Deintercalation: Synthesis and Characterization of the Nickel(I) Oxide LaNiO2, J. Am. Chem. Soc. 1999, **121**, 8843 (1999).
[12] A. Ikeda, T. Manabe, M. Naito, Improved conductivity of infinite-layer $LaNiO_2$ thin films by metal organic decomposition, Physica C **495**, 134 (2013)..
[13] K.-W. Lee and W.E. Pickett, Infinite-layer $LaNiO_2$: Ni^{1+} is not Cu^{2+}, Phys. Rev. B **70**, 165109 (2004).
[14] V. I. Anisimov, D. Bukhvalov, and T. M. Rice, Electronic structure of possible nickelate analogs to the cuprates, Phys. Rev. B **59**, 7901 (1999).
[15] Danfeng Li, Kyuho Lee, Bai Yang Wang, Motoki Osada, Samuel Crossley, Hye Ryoung Lee, Yi Cui, Yasuyuki Hikita & Harold Y. Hwang, Superconductivity in an infinite-layer nickelate, Nature **572**, 624 (2019).
[16] D. Li, B. Y. Wang, K. Lee, S. P. Harvey, M. Osada, B. H. Goodge, L. F. Kourkoutis, H. Y. Hwang, Superconducting Dome in $Nd_{1-x}Sr_xNiO_2$ Infinite Layer Films, Phys. Rev. Lett. **125**, 027001 (2020).
[17] Shengwei Zeng, Chi Sin Tang, Xinmao Yin, Changjian Li, Mengsha Li, Zhen Huang, Junxiong Hu, Wei Liu, Ganesh Ji Omar, Hariom Jani, Zhi Shiuh Lim, Kun Han, Dongyang Wan, Ping Yang, Stephen John Pennycook, Andrew T. S. Wee, and Ariando Ariando, Phase diagram and superconducting dome of infinite-layer $Nd_{1-x}Sr_xNiO_2$ thin films, Phys. Rev. Lett. **125**, 147003 (2020).
[18] M. Osada, B Y. Wang, B. H. Goodge, K. Lee, H. Yoon, K. Sakuma, D. Li, M. Miura, L. F. Kourkoutis, H. Y. Hwang, A superconducting praseodymium nickelate with infinite layer structure, Nano Lett. **20**, 5735 (2020).
[19] A.S. Botana and M.R. Norman, Similarities and Differences between $LaNiO_2$ and $CaCuO_2$ and Implications for Superconductivity, Phys. Rev. X **10**, 011024 (2020).
[20] M.-Y. Choi, K.-W. Lee and W.E. Pickett, Role of 4f states in infinite-layer $NdNiO_2$, Phys. Rev. B **101**, 020503(R) (2020).
[21] V. Olevano, F. Bernardini, X. Blase, and A. Cano, Ab initio many-body GW correlations in the electronic structure of $LaNiO_2$, Phys. Rev. B **101**, 161102(R) (2020).
[22] Y. Nomura, M. Hirayama, T. Tadano, Y. Yoshimoto, K. Nakamura, and R. Arita, Formation of a two-dimensional single-component correlated electron system and band engineering in the nickelate superconductor $NdNiO_2$, Phys. Rev. B **100**, (2019).
[23] Z. Liu, Z. Ren, W. Zhu, Z. Wang and J. Yang, Electronic and magnetic structure of infinite-layer $NdNiO_2$: trace of antiferromagnetic metal, npj Quantum Materials **5**:31 (2020).
[24] J. Gao, Z. Wang, C. Fang, H. Weng, Electronic structures and topological properties in nickelates $Ln_{n+1}Ni_nO_{2n+2}$, arXiv:1909.04657 (2019).
[25] M. Hepting, D. Li, C. J. Jia, H. Lu, E. Paris, Y. Tseng, X. Feng, M. Osada, E. Been, Y. Hikita, Y.-D. Chuang, Z. Hussain, K. J. Zhou, A. Nag, M. Garcia-Fernandez, M. Rossi, H. Y. Huang, D. J. Huang, Z. X. Shen, T. Schmitt, H. Y. Hwang, B. Moritz, J. Zaanen, T. P. Devereaux & W. S. Lee, Electronic structure of the parent compound of superconducting infinite-layer nickelates, Nature Materials **19**, 381 (2020).
[26] E. Been, W.-S. Lee, H. Y. Hwang, Y. Cui, J. Zaanen, T. Devereaux, B. Moritz, C. Jia, Theory of Rare-earth Infinite Layer Nickelates, arXiv:2002.12300 (2020).
[27] Y. Gu, S. Zhu, X. Wang, J. Hu and H. Chen, A substantial hybridization between correlated Ni-d orbital and itinerant electrons in infinite-layer nickelates, Communications Physics **3**, 84 (2020).
[28] L. Si, W. Xiao, J. Kaufmann, J. M. Tomczak, Y. Lu, Z. Zhong, and K. Held, Topotactic Hydrogen in Nickelate Superconductors and Akin Infinite-Layer Oxides ABO_2, Phys. Rev. Lett. **124**, 166402 (2020).
[29] M. Jiang, M. Berciu, and G. A. Sawatzky, Critical Nature of the Ni Spin State in Doped $NdNiO_2$, Phys. Rev. Lett. **124**, 207004 (2020).
[30] F. Lechermann, Late transition metal oxides with infinite-layer structure: Nickelates versus cuprates, Phys. Rev. B **101**, 081110(R) (2020).
[31] L.H. Hu and C. Wu, Two-band model for magnetism and superconductivity in nickelates, Phys. Rev. Research **1**, 032046 (2019).
[32] Y.-H. Zhang and A. Vishwanath, Type–II t–J model in superconducting nickelate $Nd_{1-x}Sr_xNiO_2$, Phys. Rev. Research 2, 023112 (2020).
[33] J. Karp, A. S. Botana, M. R. Norman, H. Park, M. Zingl and A. Millis, Many-body Electronic Structure of NdNiO2 and CaCuO2, Phys. Rev. X **10**, 021061 (2020).
[34] F. Lechermann, Multiorbital processes rule the $Nd_{1-x}Sr_xNiO_2$ normal state, Phys. Rev. X **10**, 041002 (2020).
[35] P. Werner and S. Hoshino, Nickelate superconductors: Multiorbital nature and spin freezing, Phys. Rev. B **101**, 041104(R) (2020).
[36] F. Petocchi, V. Christiansson, F. Nilsson, F. Aryasetiawan, and P. Werner, Normal state of $Nd_{1-x}Sr_xNiO_2$ from self-consistent GW+EDMFT, arXiv:2006.00394.
[37] M.-Y. Choi, W. E. Pickett and K.-W. Lee, Fluctuation–frustrated flat band instabilities in NdNiO2, Phys. Rev. Research **2**, 033445 (2020).
[38] X. Wu, D. D. Sante, T. Schwemmer, W. Hanke, H. Y.

Hwang, S. Raghu, and R. Thomale, Robust $d_{x_2-y_2}$–wave superconductivity of infinite–layer nickelates, Phys. Rev. B **101**, 060504(R) (2020).

[39] H. Sakakibara, H. Usui, K. Suzuki, T. Kotani, H. Aoki, K. Kuroki, Model construction and a possibility of cuprate-like pairing in a new d^9 nickelate superconductor (Nd,Sr)NiO_2, Phys. Rev. Lett. **125**, 077003 (2020).

[40] Byungkyun Kang, Corey Melnick, Patrick Semon, Gabriel Kotliar, Sangkook Choi, Infinite–layer nickelates as Ni–e_g Hund's metals, arXiv:2007.14610.

[41] Z.-J. Lang, R. Jiang, W. Ku, Where do the doped hole carriers reside in the new superconducting nickelates?, arXiv:2005.00022 (2020).

[42] M. Kitatani, L. Si, O. Janson, R. Arita, Z. Zhong, K. Held, Nickelate superconductors – a renaissance of the one-band Hubbard model, npj Quantum Materials **5**, 59 (2020).

[43] I. Leonov, S. L. Skornyakov, and S. Y. Savrasov, Lifshitz transition and frustration of magnetic moments in infinite-layer $NdNiO_2$ upon hole doping, Phys. Rev. B **101**, 241108(R) (2020).

[44] G.-M. Zhang, Y.-F. Yang, and F.-C. Zhang, Self-doped Mott insulator for parent compounds of nickelate superconductors, Phys. Rev. B **101**, 020501(R) (2020).

[45] E. M. Nica, J. Krishna, R. Yu, Q. Si, A. S. Botana, O. Erten, Theoretical investigation of superconductivity in trilayer square-planar nickelates, Phys. Rev. B **102**, 020504 (2020).

[46] T. Zhou, Y. Gao, Z. D. Wang, Spin excitations in nickelate superconductors, Sci. China-Phys. Mech. Astron. **63**, 287412(2020).

[47] Changjiang Liu, Vincent F. C. Humbert, Terence M. Bretz-Sullivan, Gensheng Wang, Deshun Hong, Friederike Wrobel, Jianjie Zhang, Jason D. Hoffman, John E. Pearson, J. Samuel Jiang, Clarence Chang, Alexey Suslov, Nadya Mason, M. R. Norman & Anand Bhattacharya, Observation of an antiferromagnetic quantum critical point in high–purity $LaNiO_3$, Nature Commun. **11**, 1402 (2020).

[48] Ying Fu, Le Wang, Hu Cheng, Shenghai Pei, Xuefeng Zhou, Jian Chen, Shaoheng Wang, Ran Zhao, Wenrui Jiang, Cai Liu, Mingyuan Huang, XinWei Wang, Yusheng Zhao, Dapeng Yu, Fei Ye, Shanmin Wang, Jia-Wei Mei, Core–level x–ray photoemission and Raman spectroscopy studies on electronic structures in Mott–Hubbard type nickelate oxide $NdNiO_2$, arXiv:1911.03177 (2020).

[49] Yi Cui, C. Li, Q. Li, Xiyu Zhu, Z. Hu, Yi–feng Yang, J. S. Zhang, Rong Yu, Hai–Hu Wen, and Weiqiang Yu, NMR Evidence of Antiferromagnetism in $Nd_{0.85}Sr_{0.15}NiO_2$, arXiv:2011.09610.

[50] H. Zhang, L. Jin, S. Wang, B. Xi, X. Shi, F. Ye, and J.-W. Mei, Effective Hamiltonian for nickelate oxides $Nd_{1-x}Sr_xNiO_2$, Phys. Rev. Research **2**, 013214 (2020).

[51] S. Ryee, H. Yoon, T. J. Kim, M. Y. Jeong, and M. J. Han, Induced magnetic two–dimensionality by hole doping in the superconducting infinite-layer nickelate $Nd_{1-x}Sr_xNiO_2$, Phys. Rev. B **101**, 064513 (2020).

[52] Y. Nomura, T. Nomoto, M. Hirayama, R. Arita, Magnetic exchange coupling in cuprate–analog d^9 nickelates, Phys. Rev. Research **2**, 043144 (2020).

[53] X. Wan, Q. Yin, and S. Y. Savrasov, Calculation of Magnetic Exchange Interactions in Mott-Hubbard Systems, Phys. Rev. Lett. **97**, 266403 (2006).

[54] A. I. Liechtenstein, M. I. Katsnelson, V. P. Antropov, and V. A. Gubanov, Local spin density functional approach to the theory of exchange interactions in ferromagnetic metals and alloys, J. Magn. Magn. Mater. **67**, 65 (1987).

[55] X. Wan, J. Zhou, and J. Dong, The Electronic Structures and Magnetic Properties of Perovskite Ruthenates from Constrained Orbital-Hybridization Calculations, Europhys. Lett. **92**, 57007 (2010); Y. Du, H. Ding, L. Sheng, S. Y. Savrasov, X. Wan and C. Duan, Microscopic origin of stereochemically active lone pair formation from orbital selective external potential calculations, J. Phys.: Condens. Matter **26**, 025503 (2014).

[56] P. Jiang, L. Si, Z. Liao, and Z. Zhong, Electronic structure of rare-earth infinite-layer $RNiO_2$(R=La,Nd), Phys. Rev. B **100**, 201106(R) (2019).

[57] S. Y. Savrasov, Linear–response theory and lattice dynamics: A muffin-tin-orbital approach, Phys. Rev. B **54**, 16470 (1996).

[58] V. I. Anisimov, F. Aryasetiawan, and A. I. Lichtenstein, Firstprinciples calculations of the electronic structure and spectra of strongly correlated systems: The LDA+U method, J. Phys. Condens. Matter **9**, 767 (1997).

[59] See Supplemental Material for additional results, supporting our conclusions.

[60] X. Wan, T. A. Maier, and S. Y. Savrasov, Calculated magnetic exchange interactions in high-temperature superconductors, Phys. Rev. B **79**, 155114 (2009).

[61] Z.P. Yin, S. Lebegue, M.J. Han, B.P. Neal, S.Y. Savrasov and W.E. Pickett, Electron–hole symmetry and magnetic coupling in antiferromagnetic LaFeAsO, Phys. Rev. Lett. **101**, 047001 (2008); M.J. Han, Q. Yin, W.E. Pickett, S.Y. Savrasov, Anisotropy, Itineracy, and Magnetic Frustration in High–T_C Iron Pnictides, Phys. Rev. Lett. **102**, 107003 (2009).

[62] X. Wan, J. Dong, and S. Y. Savrasov, Mechanism of magnetic exchange interactions in europium monochalcogenides, Phys. Rev. B **83**, 205201 (2011).

[63] R. Nanguneri and S.Y. Savrasov, Exchange constants and spin waves of the orbital–ordered noncollinear spinel MnV_2O_4, Phys. Rev. B **86**, 085138 (2012).

[64] D. Wang, X. Bo, F. Tang, and X. Wan, Calculated magnetic exchange interactions in the Dirac magnon material Cu_3TeO_6, Phys. Rev. B **99**, 035160 (2019).

[65] J. Q. Lin, P. Villar Arribi, G. Fabbris, A. S. Botana, D. Meyers, H. Miao, Y. Shen, D. G. Mazzone, J. Feng, S. G. Chiuzbaian, A. Nag, A. C. Walters, M. Garcia-Fernandez, Ke-Jin Zhou, J. Pelliciari, I. Jarrige, J. W. Freeland, Junjie Zhang, J. F. Mitchell, V. Bisogni, X. Liu, M. R. Norman, M. P. M. Dean, Strong Superexchange in a $d^{9-\delta}$ Nickelate Revealed by Resonant Inelastic X-Ray Scattering, arXiv:2008.08209.

[66] G. Kotliar, S. Y. Savrasov, K. Haule, V. S. Oudovenko, O. Parcollet, C.A. Marianetti, Electronic Structure Calculations with Dynamical Mean-Field Theory, Rev. Mod. Phys. **78**, 865 (2006).

[67] K. Haule, Quantum Monte Carlo impurity solver for cluster dynamical mean-field theory and electronic structure calculations with adjustable cluster base, Phys. Rev. B **75**, 155113 (2007).

[68] F. Ronning, K. M. Shen, N. P. Armitage, A. Damascelli, D. H. Lu, Z.-X. Shen, L. L. Miller, and C. Kim, Anomalous high-energy dispersion in angle-resolved photoemission spectra from the insulating cuprate $Ca_2CuO_2Cl_2$, Phys. Rev. B **71**, 094518 (2005); D. S. Inosov, J. Fink, A.

A. Kordyuk, S. V. Borisenko, V. B. Zabolotnyy, R. Schuster, M. Knupfer, B. Büchner, R. Follath, H. A. Dürr, W. Eberhardt, V. Hinkov, B. Keimer, and H. Berger, Momentum and Energy Dependence of the Anomalous High-Energy Dispersion in the Electronic Structure of High Temperature Superconductors, Phys. Rev. Lett. **99**, 237002 (2007).

[69] Q. Yin, A. Gordienko, X. Wan, S. Y. Savrasov, Calculated Momentum Dependence of Zhang-Rice States in Transition Metal Oxides, Phys. Rev. Lett. **100**, 066406 (2008).

[70] Y. Xiang, Q. Li, Y. Li, H. Yang, Y. Nie, H.-H. Wen, Magnetic transport properties of superconducting $Nd_{1-x}Sr_xNiO_2$ thin films, arXiv:2007.04884 (2020).

[71] M. Rossi, H. Lu, A. Nag, D. Li, M. Osada, K. Lee, B. Y. Wang, S. Agrestini, M. Garcia-Fernandez, Y.-D. Chuang, Z. X. Shen, H. Y. Hwang, B. Moritz, Ke-Jin Zhou, T. P. Devereaux, W. S. Lee, Orbital and Spin Character of Doped Carriers in Infinite-Layer Nickelates, arXiv:2011.00595.